Heliyon 10 (2024) e33356

Contents lists available at ScienceDirect

Heliyon

journal homepage: www.cell.com/heliyon

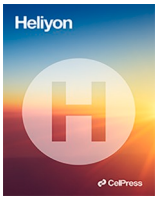

Research article

Luciferase transduction and selection protocol for reliable *in vivo* bioluminescent measurements in cancer research

Natacha Dehaen [a,b], Matthias Van Hul [b,e], Lionel Mignion [a,c], Axell-Natalie Kouakou [a,b,d], Patrice D. Cani [b,e,f,1,**], Bénédicte F. Jordan [a,c,1,*]

[a] *Biomedical Magnetic Resonance group (REMA), Louvain Drug Research Institute (LDRI), UCLouvain, Université catholique de Louvain, Brussels, Belgium*
[b] *Metabolism and Nutrition Research Group (MNUT), Louvain Drug Research Institute (LDRI), UCLouvain, Université catholique de Louvain, Brussels, Belgium*
[c] *Nuclear and Electron Spin Technologies (NEST) Platform, Louvain Drug Research Institute (LDRI), UCLouvain, Université catholique de Louvain, Brussels, Belgium*
[d] *Bioanalysis and Pharmacology of Bioactive Lipids (BPBL), Louvain Drug Research Institute (LDRI), UCLouvain, Université catholique de Louvain, Brussels, Belgium*
[e] *Walloon Excellence in Life Sciences and BIOtechnology (WELBIO), WELBIO department, WEL Research Institute, Wavre, Belgium*
[f] *Institute of Experimental and Clinical Research (IREC), UCLouvain, Université catholique de Louvain, Brussels, Belgium*

A R T I C L E I N F O

Keywords:
Bioluminescence imaging
Luciferase
Transduction
In vivo monitoring of metastasis

A B S T R A C T

Bioluminescence imaging has become an essential non-invasive tool in cancer research for monitoring various cellular processes and tumor progression *in vivo*. In this article, we aimed to propose a transduction and selection protocol for reliable *in vivo* bioluminescent measurements in immunocompetent mouse models. Using two different heterogenous luciferase-expressing cell models, we underlined factors influencing transduction. The protocol was tested through an *in vitro* luciferase activity assay as well as using *in vivo* longitudinal monitoring of metastases formation (In Vivo Imaging System®). The data were cross validated with histological assessment. Our results demonstrated stable and proportional *in vitro* and *in vivo* bioluminescent signals correlating with actual metastatic burden. Furthermore, *ex vivo* analysis confirmed the accuracy of bioluminescent imaging in quantifying metastatic surface area. This protocol should ensure reliable and reproducible measurements in cancer research utilizing luciferase-positive cell lines, confirming the validity and accuracy of preclinical studies in immunocompetent models.

1. Introduction

Bioluminescence imaging (BLI) is widely used as a non-invasive *in vivo* tool to monitor cell processes, tissues and organs. Bioluminescence is generated via enzymatic reaction through the conversion of chemical energy into light in living organisms without

* Corresponding author. Biomedical Magnetic Resonance group (REMA), Louvain Drug Research Institute (LDRI), UCLouvain, Université catholique de Louvain, Av. E. Mounier, 73 B1.73.08, 1200-Brussels, Belgium.
** Corresponding author. Metabolism and Nutrition Research Group (MNUT), Louvain Drug Research Institute (LDRI), UCLouvain, Université catholique de Louvain, Av. E. Mounier, 73 B1.73.11, 1200-Brussels, Belgium.
E-mail addresses: patrice.cani@uclouvain.be (P.D. Cani), benedicte.jordan@uclouvain.be (B.F. Jordan).
[1] co-senior authors and co-corresponding authors

https://doi.org/10.1016/j.heliyon.2024.e33356
Received 9 April 2024; Received in revised form 17 June 2024; Accepted 19 June 2024
Available online 23 June 2024

excitation source [1]. For that purpose, luciferase, which can catalyze the reaction with its substrate luciferin and generate bioluminescence, is introduced into living organisms where the luciferase gene is integrated into the cell chromosome. This method has been applied to assess tumor growth [2], bacterial and virus infection [3], protein-protein interaction [4] and transgenes [5].

Specifically, within cancer research, BLI finds extensive use in evaluating tumorigenesis, metastases, metabolic processes, apoptosis, hypoxia, angiogenesis, and the efficacy of cancer therapies [2]. BLI is considered as a pivotal imaging modality in preclinical cancer research since commonly used animal models have no intrinsic bioluminescence, meaning that the background signal is close to zero, thereby surpassing many other modalities in terms of sensitivity and allowing a relative measurement [2]. The downside of this approach is that it necessitates conducting the technique either in transgenic animals, i.e. by inserting the specific luciferase reporter gene to obtain luciferase expression *in vivo*, or by injection of the transfected or virally transduced cancer cells into the animal's body [2]. As genes for luciferase are duplicated upon cell division the technique is sensitive to cell proliferation, enabling the longitudinal monitoring of primary or metastatic tumor growth. However, the technique is by essence only reliable if the expression is stable over time.

As a matter of fact, the transduction and selection protocols are of the utmost importance. In the literature, conflicting findings have been observed. These discrepancies might potentially be due to protocol variations. For instance, Baussart et al. [6] reported a discrepancy between BLI and Magnetic Resonance Imaging (MRI) in glioblastoma growth evaluation. Despite a brain tumor being detected by MRI, they observed a loss of bioluminescent signal *in vivo*, suggesting viral construction as the cause. In other studies, concerns arised regarding the potential toxicity and immunogenicity of green fluorescent protein, green fluorescent protein (GFP), in immunocompetent mice such as the C57BL/6 model. Post transduction GFP toxicity could weaken cells and hinder metastatic growth due to their fragility [7–9]. As metastasis represents an inefficient process, with only 0.01 % of cells intravasating into circulation capable of forming detectable metastases [10], pre-existing fragility may limit the success of such a model. Furthermore, GFP may trigger immune responses, causing challenges in immunocompetent mouse models [7,8]. A last but not less important aspect is the cellular heterogeneity. Although several studies in oncology utilize luciferase-expressing clones to ensure uniform bioluminescence intensity [11–13], the role of cellular heterogeneity in tumors is recognized as a major factor causing tumor relapse and metastasis. It has also been shown that human metastases consist of heterogeneous, polyclonal cells [14]. It is therefore more relevant to work with polyclonal populations in oncological studies.

Although we recently utilized a widely accepted transduction protocol, regarded as a standard in the field, to transduce the Py8119 murine breast cancer cell line [15] with a lentiviral vector co-expressing luciferase and GFP, we experienced many issues. Indeed, after injection of transduced Py8119 cells into C57BL/6JRj mice, the *in vivo* signal was unstable over time and was not proportional to the tumor size, regardless to the route of injection (tail vein, intracardiac) or the tumor localization (orthotopic or metastatic) (Supplementary Fig. 1). This lack of correlation between the *in vivo* bioluminescent signal and the actual tumor size estimated *ex vivo* using H&E staining might potentially be due to a heterogeneous *in vitro* transduced population (non transduced vs transduced), despite the use of a lentiviral transduction and a selection process that was previously validated in other cell lines [16]. In addition, most of the published protocols are used in immunodeficient mice. However, as GFP might be immunogenic, it can constitute an issue when using immunocompetent mice.

To address the unmet need in the field, the main objective of our study was to develop a transduction and selection protocol that ensures reliable *in vivo* bioluminescent measurements in immunocompetent mice. We aimed to maintain the authenticity of the tumor by using a heterogeneous cell line instead of clones. This approach should allow researchers to work under suitable experimental conditions, facilitating longitudinal monitoring of metastasis formation *in vivo*, particularly in the lungs, while overcoming major challenges such as signal loss due to viral constructs, the potential toxicity and immunogenicity of GFP.

2. Materials & methods

2.1. Technical note

2.1.1. Cell lines

HEK 293T cells, derivative human cell line that expresses a mutant version of the SV40 large T antigen, were kindly provided by T. Michiels (De Duve Institute, UCLouvain, Brussels) and used to produce lentiviruses. 293T cells were cultured in Dulbecco's modified Eagle medium (DMEM) (Lonza, Walkersville, MD, USA) supplemented with 10 % of fetal calf serum (FCS, Sigma), 100 U/ml penicillin and 100 μg/ml streptomycin (Thermo Fisher).

To develop the various *in vitro* and *in vivo* protocols, we worked with two different cancer cell line models, namely Py8119 breast cancer cells (ATCC-CRL-3728, ATCC, Manassas, VA, USA) and YUMM1.7 melanoma cells (ATCC-CRL-3362, ATCC, Manassas, VA, USA).

Py8119 *Mus musculus* mammary gland adenocarcinoma and YUMM1.7 *Mus musculus* malignant melanoma cell lines were stored according to the American Type Cell Culture (ATCC, Manassas, VA, USA). Py8119 cells were cultured in F–12K medium (GIBCO, Thermo Fisher Scientific, Waltham, MA, USA) with 7 mM glucose and 2 mM glutamine, supplemented with 5 % heat inactivated fetal bovine serum (FBS, Thermo Fisher Scientific, Waltham, MA, USA). YUMM1.7 cells were maintained in culture in Dulbecco's Modified Eagle Medium/Nutrient Mixture F-12 (DMEM-F12, GIBCO, Thermo Fisher Scientific, Waltham, MA, USA) supplemented with 10 % heat inactivated FBS (GIBCO, Thermo Fisher Scientific, Waltham, MA, USA). Both cell lines were incubated in a humidified atmosphere at 37 °C and 5 % CO_2.

2.1.2. Transduction and selection (Fig. 1)

Plasmid TM915 (pTM915, Supplementary Fig. 2) was kindly provided by T. Michiels (De Duve Institute, UCLouvain, Brussels). This plasmid was obtained by cloning the firefly coding sequence in pTM900 [17]. This construct carries a self-inactivating, third generation lentiviral vector derived from the pCCLsin.PPT.hPGK.GFP.pre. construct [18]. In the pTM915 construct, the luciferase (Luc) gene is expressed under the same promotor, hPGK (human Phosphoglycerate Kinase), as the Hygromycin B antibiotic resistance gene (HygR), which will be useful during selection. This dual expression is made possible by the presence of an Internal Ribosome Entry Site (IRES) sequence between the two genes of interest. IRES facilitates simultaneous expression of luciferase and antibiotic resistance genes under the same promoter by allowing ribosomes to start translation internally. This ensures coordinated functionality, crucial for experimental setups requiring simultaneous gene expression during the selection process [19].

Lentiviruses were produced in HEK 293T cells as in Lizcano-Perret et al., 2022 [20], by co-transfection of the following plasmid, using TransIT-LT1 reagent (Mirus Bio): 2.5 μg of lentiviral vector pTM915, 0.75 μg of pMD2-VSV-G (VSV-glycoprotein), 1.125 μg of pMDLg/pRRE (Gag-Pol), and 0.625 μg of pRSV-Rev (Rev). DNA quantities are for transfection of 1 well of a 6-well plate. Supernatants were typically collected 72 h post transfection and filtered (porosity: 0.45 μM). An additional step of centrifugation was applied to concentrate and purify the lentiviral vector. Centrifugation was performed at 4°c, for 4 h, at 10000 g through a 10 % sucrose cushion (50 mM Tris HCl_2 pH 7,4, 100 mM NaCl, 0,5 mM EDTA (Ethylenediaminetetraacetic Acid), 10 % sucrose).

For transduction, cells were typically seeded in a 24-well plate (Thermo Scientific ™, product number 142485) to obtain a density of 5000–10,000 cells/well and infected 2 times in 48 h with 150 μL of filtered lentivirus or with 50 μl of concentrated lentivirus. Half of the medium was renewed 24 h after the first infection. When the cells were confluent, they were passaged to a well with a larger surface area (6 wells, VWR, 734–2323). This was done by first rinsing the well with 500 μl of PBS (Phosphate Buffered Salin at pH 7.4, Thermo Scientific, 10010023) and then detaching the cells from the well surface using 500 μl of trypsin-EDTA 0.05 % phenol red (Thermo Fischer Scientific, 25300-054) at 37 °C for 3 min. The trypsin was neutralized with 1 ml of culture medium and the cells were transferred to a 6-well plate. Antibiotic selection was then started by adding 300–400 μg/ml Hygromycin B (Roche, ref. 10843555001) to the medium. The luciferase gene is associated with a gene for resistance to hygromycin B. Only the cells that were effectively transduced will survive at this stage. This is why antibiotic selection follows the initial passage before amplification.

Finally, the transduced cells were amplified in the presence of hygromycin B. All manipulations were carried out under a L2 biosafety flow.

2.1.3. Luciferase activity assay

Py8119 luciferase, YUMM1.7 luciferase and wildtype cells were seeded (90 000 cells/well to reach a confluence of + -50 % after 24 h) in 24-well plates (Thermo Scientific ™,142485). After 24 h, the medium was aspirated and the cells rinsed with 500 μl/well of cold PBS at 4 °C (Phosphate Buffered Saline pH 7.4, Thermo Scientific, 10010023). The luciferase activity assay was performed using the Promega E1501 Luciferase Assay System. Next, the lysis buffer (Promega kit, Luciferase Cell Culture Lysis 5X Reagent, E1531) was prepared in sterile water (dilution factor, 1:5). 100 μl/well of lysis buffer (1×) was added to each well and the cells were incubated for 15 min on a shaker plate at room temperature. In parallel, sterile tubes containing 25 μl of luciferase substrate (E151A) were prepared for addition of 8 μl cell lysate prior to luminometer (Promega, Glomax, 20/20) reading of the bioluminescent signal. Steps were repeated for 3 wells/cell line to have triplicates per cell line and the experiment was repeated 3 times at 3 different timings.

2.1.4. In Vivo Imaging System®

The study was conducted according to the guidelines of the Declaration of Helsinki and approved by the ethical committee for animal care of the Health Sector of the Université Catholique de Louvain, under the supervision of JP Dehoux, under the specific numbers 2023/UCL/MD/10 and 2023/UCL/MD/A20, and performed in accordance with the guidelines of the local ethics committee and in accordance with the Belgian Law of 29 May 2013, regarding the protection of laboratory animals (agreement number LA1230467).

C57BL/6JRj immunocompetent female and male mice were used with a black fur. To avoid bias from hair color and thickness that may affect BLI results, therefore the area of interest, specifically the torso (where the lungs are located), was shaved to mitigate this potential bias. The drawbacks of BLI include poor spatial resolution, limited penetration depth, and diminished quantification accuracy due to loss and scatter of light in the body. These limitations have hindered effective visualization of internal organs of animal and have thus precluded potential clinical translation [21,22].

200 000 freshly passaged Py8119 Luciferase and 500 000 freshly passaged YUMM1.7 luciferase (ATCC, Manassas, VA, USA) cells diluted in 150 μl of HBSS (Hank's Balanced Salt Solutions, ATCC, 30–2213) were injected within 30 min of detachment (put into solution) intravenously in C57BL/6Jrj 13 weeks-old mice (Janvier labs, France). Py8119 luciferase cells were injected in 8 female mice and YUMM1.7 luciferase cells in 4 male mice. Lung metastases in mice were monitored at least once a week with the IVIS® (In Vivo Imaging System®, PerkinElmer). To do so, mice were anesthetized by isoflurane inhalation (2.5 % in air for sleep induction and 1,5 % in air during the monitoring of ± 30 min) and 100 μl of the substrate of luciferase, XenoLight D Luciferin-K + Salt Bioluminescent Substrate (PerkinElmer, ref. 122799) was injected intraperitoneally at a concentration of 40 mg/ml. Injections were done alternately on the right and on the left side of the mouse's peritoneum. The body temperature of the mice was maintained at 37° C by a heating plate in the IVIS® system. IVIS® images were acquired with the following parameters: time of acquisition; automatic, 1/4-8-m-m.

To be able to compare the data from one run to another, we acquired images using identical parameter settings and under similar conditions for both cell lines (Py8119 and YUMM1.7 luciferase). The size of the ROI area (region of interest area) was maintained for all images and the total flux (expressed in photons per second (p/s)) of each mouse was compared. The negative control mouse was anesthetized and passed into the IVIS®; an IP (intraperitoneally) injection of XenoLight D Luciferin-K + Salt luciferin was performed,

but it was not injected with luciferase-positive cells.

After 28 days mice were anesthetized with isoflurane and sacrificed by cervical dislocation. Immediately after dislocation, the lungs were removed and were analyzed in the IVIS® system after 5 min immersion in a 4 mg/ml XenoLight D Luciferin-K + Salt Bioluminescent Substrate (PerkinElmer, ref. 122799) solution.

2.1.5. Hematoxylin and eosin staining

Five minutes after lung sampling and IVIS® acquisition, the lungs were immersed in paraformaldehyde (PFA Formaldehyde solution 4 % - buffered - pH 6.9, Sigma-Aldrich, ref. 1004965000) at 4 °C for fixation. The lungs were placed in paraffin within 48 h. Tissue sections were precisely cut every 250 μm at 6 different levels to obtain representative material for microscopic examination. Lung metastases were highlighted using hematoxylin and eosin staining. The percentage of metastatic surface was quantified using the Halo® software (Artificial Intelligence, Indica Labs).

2.1.6. Statistical analyses

Detailed information regarding statistical tests, sample sizes, p-value thresholds, and other specific methodological aspects are provided in the captions of the respective figures. Whenever feasible, Oneway Anova, Tukey's multiple comparisons test and non-parametric unpaired *t*-test have been utilized.

3. Results

To validate the transduction and selection protocol, we carried out *in vitro* and *in vivo* longitudinal tests in two different cell lines, Py8119 (triple negative breast cancer) and YUMM1.7 (Yale University Mouse Melanoma).

3.1. In vitro experiments

3.1.1. Transduction and selection

As shown in Fig. 1, HEK 293T cells were transfected with plasmids Beta-lactamase (Bla) and plasmid pTM915 (described in Supplementary Fig. 2), 24 h post-transfection lentivirus were collected and filtered. The cancer cells were transduced by two rounds of infection with the lentiviral vector particles. A heterogeneous population in regard to the luciferase expression was obtained. The selection of luciferase-positive cells was accomplished by the addition of the antibiotic Hygromycin B. Subsequently, luciferase-positive cells (Py8119 and YUMM1.7) were amplified for *in vitro* and *in vivo* assays.

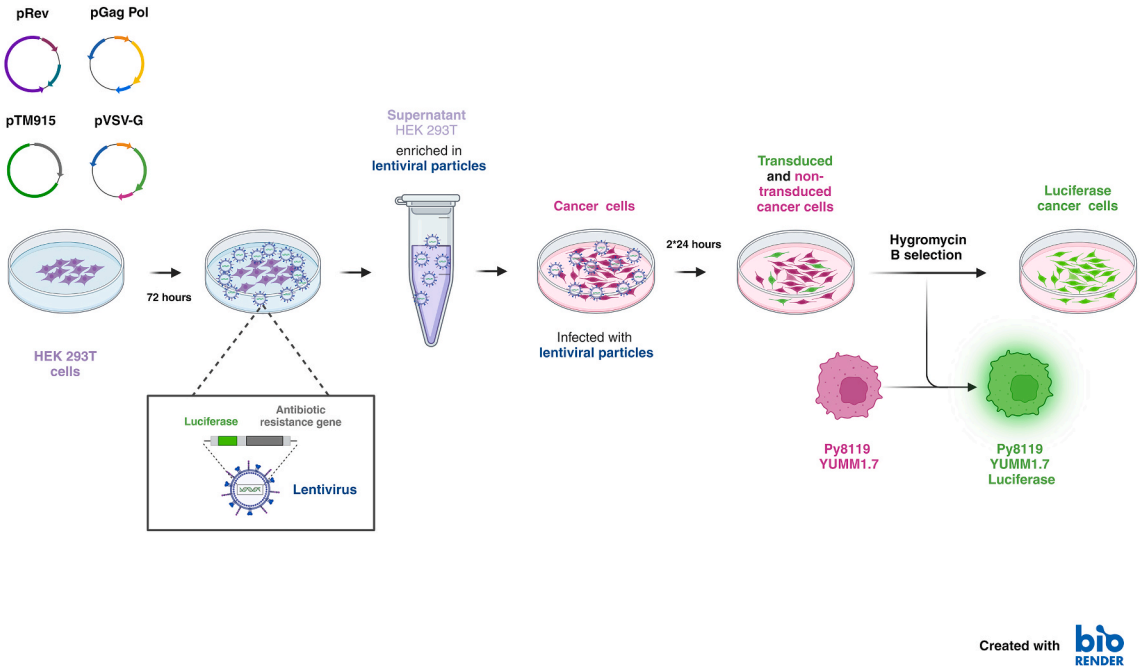

Fig. 1. Workflow from lentivirus production, infection to transduction and selection of luciferase-positive cancer cell line. In 72 h, HEK 293T cells permitted the production of lentiviruses, vectors carrying the plasmid of interest (containing the luciferase gene and the antibiotic resistance gene under the same promoter). Subsequently, the lentiviruses present in the supernatant were collected and exposed to cancer cells for two consecutive 24-h periods. This step led to the generation of a heterogeneous population in terms of luciferase expression, with some cells transduced and others not transduced (wild type cells). Treatment with hygromycin B finally enabled the selection of transduced cells.

3.1.2. *In vitro* luciferase activity

The first step was to check whether lentivirus-mediated transduction of the luciferase gene in Py8119 and YUMM1.7 cell lines was successful, using an *in vitro* luciferase activity assay. A significantly higher luciferase activity was shown in the transduced cell lines compared to the non-transduced cells, (i.e. wildtype, WT), demonstrating the efficiency of the transduction protocol in 3 different passages at 3 different timings, as shown in Fig. 2.

It's worth mentioning that the higher signal observed in the Py8119 Luc line might be the consequence of the growth rate, as Py8119 Luc cells exhibit a faster growth rate compared to YUMM1.7 Luc cells or more luciferase genes where integrated in the genome of one cell line compared to the other. Since Py8119 and YUMM1.7 wildtype cells had the same absence of bioluminescent signal *in vitro* (close to zero, less than 100 total flux (p/s)) we decided to put only one of the two negative control results in the graph.

The luciferase activity of the Py8119 Luc and YUMM1.7 Luc cell lines does not change across the different passages, and the measurements of luciferase activity was carried out under the same conditions but at different timings, corresponding to three different cell passages (n = 3). Importantly, *in vitro* luciferase activity remained stable over time.

3.2. *In vivo and ex vivo experiments*

3.2.1. *Cross-validation methods (Fig. 3[A-C])*

To validate the results obtained *in vivo* and *ex vivo*, it was decided to cross-validate them with the percentage of metastatic surface area assessed by H&E staining in mouse lungs. The aim was to demonstrate that the signal observed *in vivo,* and *ex vivo* is specific to the presence of metastases in the lungs. In Fig. 3A and B, the signal of a single mouse is illustrated in terms of *in vivo* and *ex vivo* bioluminescence, and in terms of quantified metastatic surface in the lungs (see Fig. 3C–via histological slides on 6 different levels representing the entirety of the lung).

3.2.2. *In vivo bioluminescence (Fig. 4[A-C])*

To confirm the efficacy of the transduction protocol, we checked the stability of luciferase expression by the cell line *in vivo* over time. The transduced cells were injected intravenously into C57BL/6JRj mice, and the signal was monitored over time with the IVIS® system. Longitudinal images acquisition was performed between day 7 and day 28 post tumor induction by injecting Luciferin intraperitoneally (IP) 15 min before each run (Fig. 4A and B). For both cell lines, the *in vivo* bioluminescent signal (total flux (p/s)) was stable between day 7 and day 14–15, and then increased over time until day 28, at which time mice were sacrificed for *ex vivo* quantification.

To conclude, the *in vivo* bioluminescent signal of the Py8119 luciferase cell line was higher and more stable over time than the one measured with IV injection of 500 000 Py8119 previously transduced with the luciferase and GFP co-expressing vector (see Supplementary Fig. 2).

3.3. *Ex vivo bioluminescence and H&E staining (Fig. 5[A-D])*

After collection, the lungs underwent imaging using the IVIS® system to quantify lung metastases *ex vivo* and to compare the data with those obtained with H&E staining. A comparable pattern was found when comparing the bioluminescent signal measured *ex vivo* (Fig. 5A and C), and the percentage of metastatic area quantified by H&E staining (Fig. 5B and D), the YUMM1.7 luciferase metastases displaying a stronger bioluminescent signal (in total flux (p/s)) and a higher metastatic surface per lung surface as compared to the Py8119 luciferase metastases.

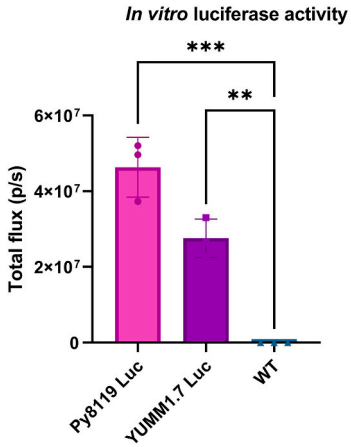

Fig. 2. Luciferase activity assay measuring total flux (p/s), in Py8119 Luciferase (Py8119 Luc), YUMM1.7 Luciferase (YUMM1.7 Luc) and wild type cells (WT). Oneway Anova, Tukey's multiple comparisons test, n = 3, each point on the graph represents one passage, and each passage was achieved at a different timing. **: $p < 0.01$, ***: $p < 0.001$.

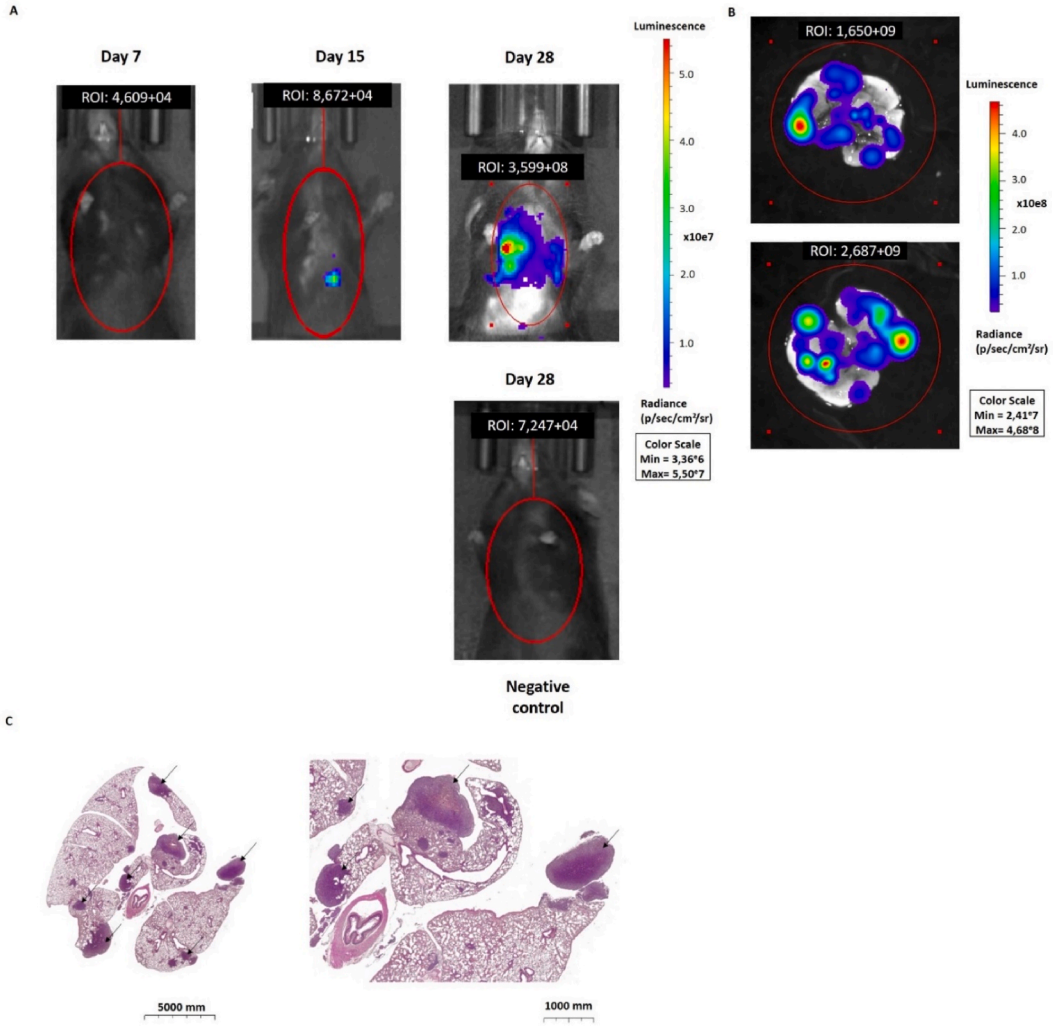

Fig. 3. Representative *in vivo* images acquired at a different timing (A) and *ex vivo* images (B) acquired by the IVIS® system showing the bioluminescent signal in the lungs and the lung staining with Hematoxylin and Eosin at different magnifications (the arrows represent metastases in the lungs) (C) of the same mice. The negative control mouse was not injected intravenously with luciferase positive cells, as mentioned in the materials and methods section.

4. Discussion

The objective of this work was to propose a transduction protocol applied to two heterogeneous cancer cell lines, to conduct *in vivo* bioluminescence experiments in immunocompetent mice to track metastasis formation. Optical imaging is indeed a potent tool for real-time observation of biological events, including two main methods: fluorescence and bioluminescence. The advantage of bioluminescence is its specificity, which minimizes background noise. There are various bioluminescent reporters, but we chose to work with firefly luciferase and its substrate luciferin, known as the gold standard for *in vivo* use [23,24].

Following several unsuccessful attempts to develop a stable luciferase and GFP-positive cell line model by applying previously published protocols to our experimental setup, concerns began to emerge regarding the universality of some extensively used methods in published literature [25,26]. Moreover, various articles have brought attention to specific challenges to consider when using these cellular tools such as the immunogenicity and toxicity of GFP [7,27], as well as the loss of luciferase expression over time [6].

To reach our objective we used a plasmid where luciferase is linked to an antibiotic-resistant gene through an IRES element, all under the control of the same human hPGK promoter. In addition, we opted to work with polyclonal, heterogenous cells *in vivo* to closely mimic tumor reality in murine models. Moreover, as the selection of the appropriate viral vector is crucial based on the cell type, we choose to use a lentiviral vector for its ability to integrate into the genome of non-dividing cells, making it suitable for targeting highly differentiated cells like the YUMM1.7 Melanoma cell line [28]. Lentiviruses indeed ensure stable genomic integration and long-term transgene expression, essential for cancer and metastasis research both *in vitro* and *in vivo*. Additionally, we validated the protocol *in vitro* and *in vivo* using another cell line, particularly the Py8119 triple-negative lineage, known for its low differentiation

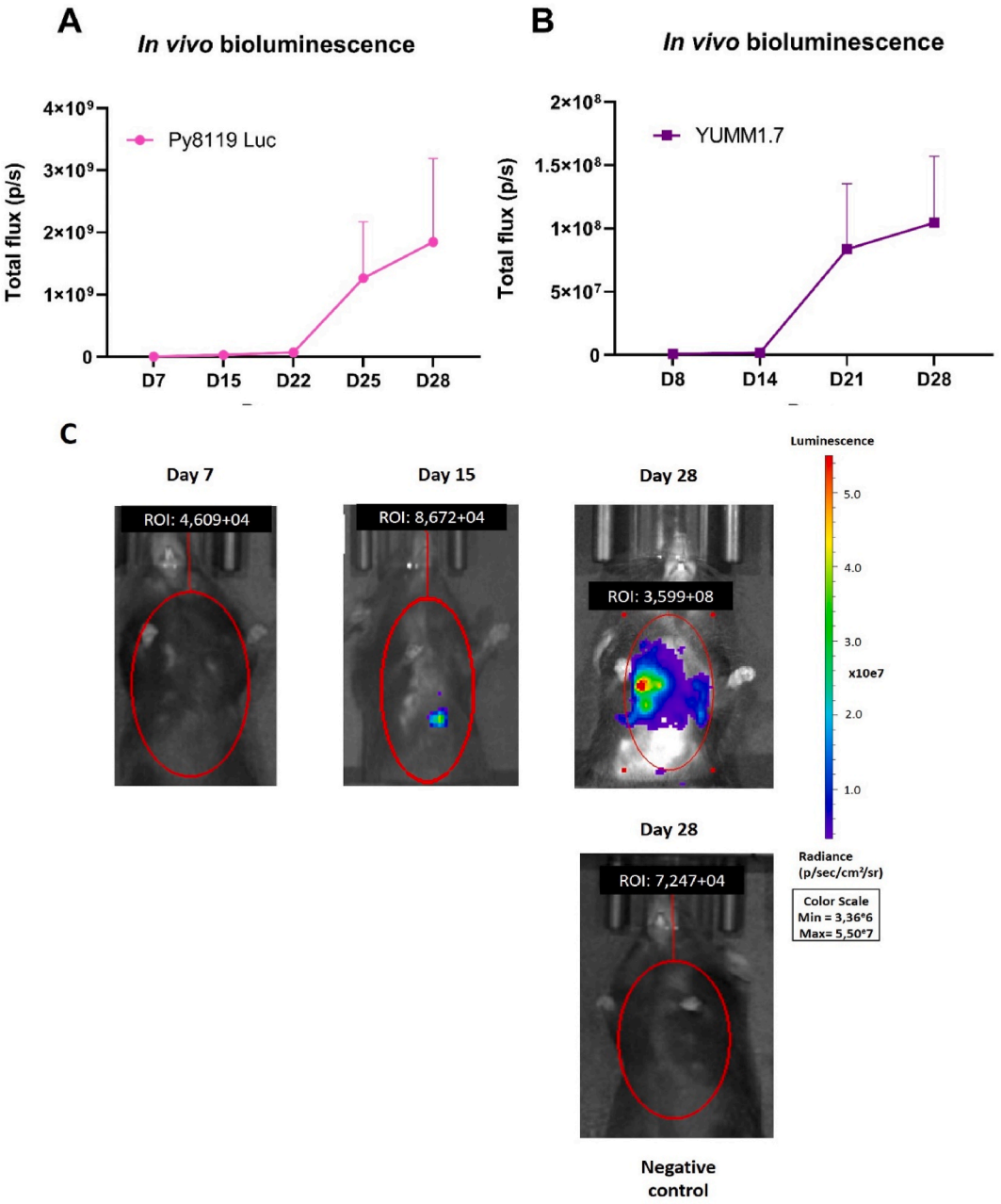

Fig. 4. A) *In vivo* longitudinal monitoring of the bioluminescent signal of Py8119 luciferase cells, n = 8. B) *In vivo* longitudinal monitoring of the bioluminescent signal of YUMM1.7 luciferase cells, n = 4. C) Representative *in vivo* images acquired at a different timing by the IVIS® system showing the bioluminescent signal in the lungs of the same mice. The negative control mouse was not injected intravenously with luciferase positive cells, as mentioned in the materials and methods section.

level [29] in order to confirm that the protocol is optimal for both highly differentiated or poorly differentiated cell lines. The importance of some key factors related to our approach is discussed below.

A first aspect to consider is that GFP is immunogenic and has been demonstrated to influence the growth and progression of metastases [8,9,27]. Since metastatic spread involves participation of the immune system, its modulation by GFP might represent a serious confounding factor, limiting the validity of data derived from such models [30]. On the contrary, luciferase allows, in this study, *in vivo* monitoring of metastases formation over time in immunocompetent C57BL/6JRj mice (male and female), owing to the emission of bioluminescence, without encountering immune system rejection issues nor impacting on the metabolism of cancer cells [31].

Prior to transduction process, a second crucial step is the choice of a suitable viral vector. For our study, the plasmid pTM915, was

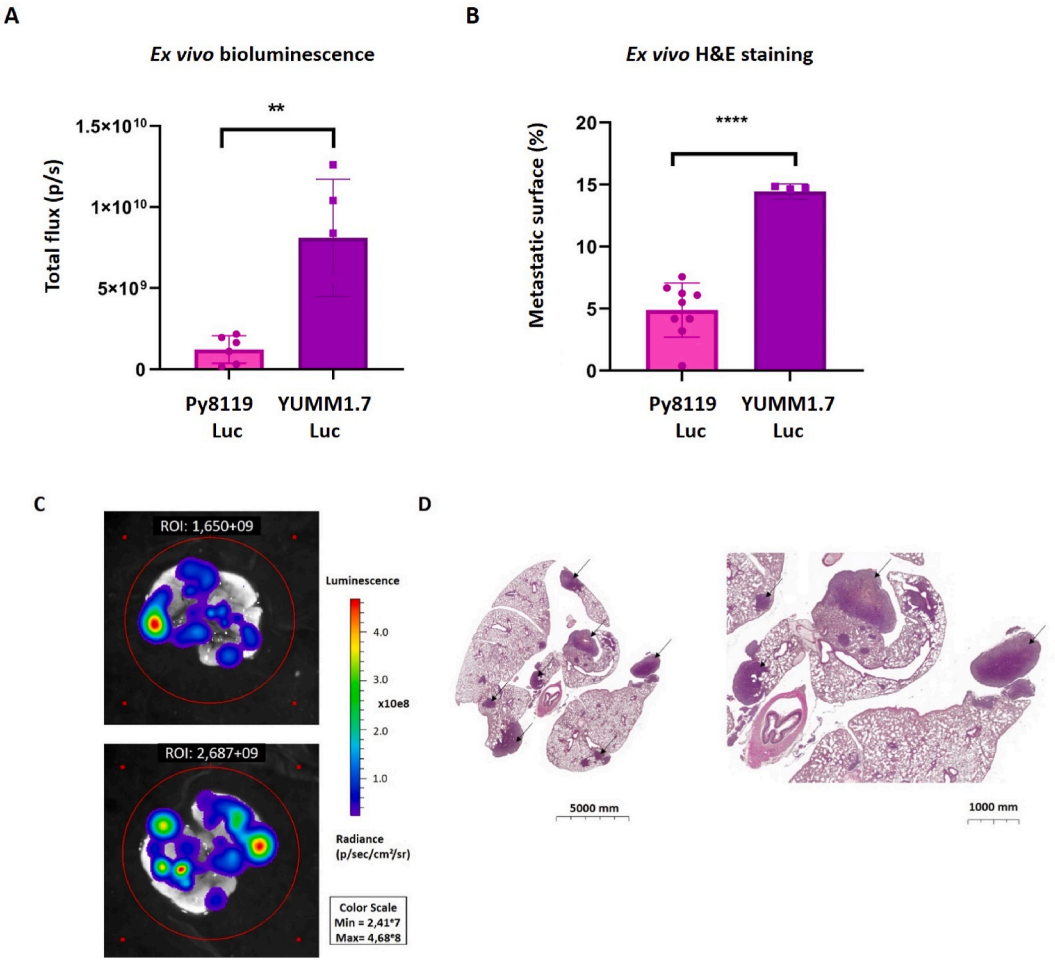

Fig. 5. A) Total flux (p/s) of the lungs measured *ex vivo* using the bioluminescence IVIS® system (Py8119 Luc n = 8, YUMM1.7 Luc n = 4). Non-parametric unpaired *t*-test, **: $p < 0.01$. B) Quantification of the percentage of the metastatic surface in the lungs (sum of percentages of 6 slides/lung) quantified on H&E staining, (Py8119 Luc n = 8, YUMM1.7 Luc n = 4). Non-parametric unpaired *t*-test, ****: $p < 0.0001$. C) *Ex vivo* images acquired by the IVIS® system showing the bioluminescent signal in the lungs. D) *Ex vivo* images of the lung staining with Hematoxylin and Eosin (at different magnifications). The arrows represent metastases in the lungs of the same mice.

selected. The structure of the plasmid was established with the promoter of human PGK. Given that PGK is ubiquitous and cells constitutively express this enzyme to sustain their energy needs, leveraging the PGK promoter ensures consistent expression of the target gene. For selection purposes, the luciferase gene was linked to an IRES, specifically for Hygromycin B, under the control of the same hPGK promoter, optimizing the identification and maintenance of successfully modified cells.

A third important and often overlooked step is the survival curve of the cells in the presence of an increasing concentration of the antibiotic used for the selection of successfully transduced cells. An excessive concentration of the antibiotic has the potential to eradicate all cells, including those that have been transduced. Accordingly, the antibiotic concentration should be sufficiently high to cause death in non-transduced WT cells while sparing transduced cells, that express the resistance gene. The fact that non-transduced WT cells would not die following antibiotic selection *in vitro* may lead to a mixed population of transduced and non-transduced cells, thereby presenting a challenge in conducting *in vivo* experiments. Non-transduced WT cells could potentially dominate *in vivo*, forming non-luciferase-positive metastases that cannot be longitudinally monitored due to the absence of a bioluminescent signal. Indeed, if the cell does not rely on luciferase for survival, unaltered cells with less impairment typically prevail *in vivo*, resulting in an IVIS® signal that does not correlate proportionally with tumor or metastases size. In this study, the selected antibiotic concentration was the one resulting in the death of all cells within 48 h.

Another step undertaken to optimize transduction was to perform a double infection, exposing the cells to lentivirus twice within 48 h, aiming to increase the chances of the cells to be infected by the lentivirus without causing cell death. Indeed, if transduction is a widely used method for obtaining a luciferase-positive cell line, the number of cells is lineage-specific (e.g., difference in cell size, growth time, non-adherent or adherent cells). In addition, a maximum confluence of 50 % after 24 h has been targeted to ensure enough cells are ready to be infected and survive the infection, while also providing enough space for cells to continue growing despite

the presence of lentivirus.

A final important point is that we refrained from using a clone to maintain the diversity present within the cancer cell population. This implies that luciferase expression varies from cell to cell. Alternatively, a set of clones with the same luciferase activity could be combined to mitigate this inherent bias. However, other biases would be introduced, such as the lack of representativeness of reality in terms of the heterogeneity of the cell population.

One limitation of our study is a potential variation in luciferase expression across different cells as our protocol allows a non-specific integration of the luciferase gene into the genome of the cancer cells. In addition, working with a heterogeneous, polyclonal cell population inherently leads to variability in luciferase activity. Monitoring metastasis *in vivo* using the IVIS® method as a longitudinally and semi-quantitative tool prevents this issue. To validate the bioluminescence results quantitatively, cross-validation with hematoxylin and eosin staining was necessary. Accordingly, after *in vivo* measurements, the lungs were imaged *ex vivo* with the IVIS® system, to eliminate potential confounding factors (*in vivo* acquisition depth for example) and account solely for metastases surface. The bioluminescent signal from the anterior and posterior surface of the lung have been acquired, with the aim of capturing the signal from both sides of the lungs. Subsequently, the two acquired signals were combined to provide an overall *ex vivo* signal. Quantification of the percentage of metastatic surface area on each lung was added to cross-validate the method and offer quantitative insights. Importantly, this quantification confirmed the correspondence of the observed signal using bioluminescent imaging to actual lung metastases.

Of note, if the bioluminescent signal in total flux (p/s) was higher in the Py8119 luciferase cell line both *in vitro* and *in vivo,* compared to the YUMM1.7 luciferase cell line, the trend was reversed *ex vivo*, as shown using both BLI and in H&E staining measurements. Different factors may explain this apparent discrepancy. First, it might be due to the fact that the proliferation rate of Py8119 luciferase cells is faster *in vitro* than that of YUMM1.7 cells. Another explanatory factor may be that Py8119 luciferase cells could have integrated more luciferase gene into their genome than YUMM1.7 luciferase cells. Besides, an important point to emphasize is that the *ex vivo* passage of the lungs to the IVIS system is impacted by the decrease in ATP due to the organ resection. In particular, as the luciferase reaction with its substrate luciferin requires oxygen, $Mg2+$ as well as ATP, the time to sacrifice the mouse and place the lung in the IVIS® system (that can take up to 5 min), can significantly impact the amount of ATP and thus the bioluminescent signal. Other factors that may impact the bioluminescent signal are not mouse model-dependent but rather related to the environment, such as hypoxia, hypoperfusion, and pH [32]. We did not study these parameters as we did not observe a decrease in signal over time with our protocol. Another important point to consider in studying metastasis formation with bioluminescence is that the target organ may influence the *in vivo* signal. This is not only due to the location or thickness (with or without black or white fur) but also the structure of the organ itself, which may potentially influence the signal, as observed with bone metastases [33]. Therefore, this must be considered when interpreting *ex vivo* bioluminescence results. Importantly, the cross-validation with *ex vivo* H&E staining shows that the bioluminescence technique is reliable to monitor lung metastatic growth within a single tumor model.

Overall, the protocol proposed in this article presents several advantages. It has been validated both *in vitro* and *in vivo* on two different cell lines, demonstrating its reproducibility. It is however important to note that adaptations may be necessary depending on the cell line, but we believe these adjustments are feasible based on the points addressed in this article. While generalizing the protocol to other models, both *in vitro* and *in vivo* tests (on a small number of animals) will need to be conducted to ensure stable luciferase-positive model before proceeding with experiments on a larger scale. Another advantage of the study is that the two cell lines were selected based on their differentiation status, showing that the protocol is optimal regardless of their differentiation state or cancer origin (triple-negative breast cancer or melanoma). Additionally, the cell population used *in vitro* and *in vivo* for both cell lines is heterogeneous in terms of luciferase expression, allowing us to avoid working with clones and thus maintain the cellular heterogeneity found in human metastases. Although polyclonal populations may not yield quantitative *in vitro* and *in vivo* results due to heterogeneity influencing signal intensity and kinetics [34], this choice did not affect the bioluminescent signal neither *in vitro* nor *in vivo.* Finally, the protocol enabled the development of two bioluminescent cell lines that could be used in immunocompetent mouse models. Since the immune system plays a crucial role in cancer development, this allowed us to work under conditions closer to reality using the C57BL/6 mouse model. Therefore, the role of the immune system is not overlooked as it is the case with immunodeficient models. Of note, the potential bias introduced by the fur color of C57BL/6 mice can be corrected by shaving the fur.

Taken into consideration the above-mentioned advantages and limitations, bioluminescence optical imaging method is considered as a semi-quantitative approach for *in vivo* metastases detection [6]. In line with this, our results show that with a well-established protocol, working with a heterogeneous cancer cell line in terms of luciferase expression *in vivo* is possible as a semi-quantitative and specific method for monitoring metastasis formation *in vivo* in immunocompetent mice.

In conclusion, to effectively create a luciferase-positive line for *in vivo* applications in immunocompetent models, it is essential to meticulously manage every aspect of the process, including cell seeding, transduction, and selection. This will help to avoid bias during both *in vitro* and *in vivo* experiments involving such a cell line. While transduction is not the sole effective method, our study offers a comprehensive and validated methodology across two cancer cell lines.

Ethics statement

The study was conducted according to the guidelines of the Declaration of Helsinki and approved by the ethical committee for animal care of the Health Sector of the Université Catholique de Louvain, under the supervision of JP Dehoux, under the specific number 2023/UCL/MD/A20 and 2023/UCL/MD/10, and performed in accordance with the guidelines of the local ethics committee and in accordance with the Belgian Law of May 29, 2013, regarding the protection of laboratory animals (agreement number LA1230467).

Data availability statement

Data will be made available on request.

Fundings

This work was supported by

* BF is Research Director from the FNRS (Fonds de la Recherche Scientifique) and ND is Televie Grant Researcher
* ARC19/24–096/Actions de Recherches concertées-Communauté Française de Belgique.
* FRFS-WELBIO: WELBIO-CR-2022A-02
* EOS: program no. 40007505.

Walloon Excellence in Lifesciences and Biotechnology.

CRediT authorship contribution statement

Natacha Dehaen: Writing – review & editing, Writing – original draft, Investigation, Formal analysis, Data curation, Conceptualization. **Matthias Van Hul:** Writing – review & editing, Project administration, Investigation. **Lionel Mignion:** Writing – review & editing, Methodology. **Axell-Natalie Kouakou:** Writing – review & editing, Resources. **Patrice D. Cani:** Writing – review & editing, Validation, Supervision, Resources, Project administration, Investigation, Funding acquisition, Data curation, Conceptualization. **Bénédicte F. Jordan:** Writing – review & editing, Validation, Supervision, Resources, Project administration, Investigation, Funding acquisition, Data curation, Conceptualization.

Declaration of competing interest

The authors declare the following financial interests/personal relationships which may be considered as potential competing interests: Patrice D. Cani reports financial support was provided by WELBIO asbl. Benedicte F. Jordan and Patrice D. Cani reports financial support was provided by Fund for Scientific Research. Patrice D. Cani was co-founder of The Akkermansia Company SA and Enterosys. Patrice D. Cani and Benedicte Jordan are coinventors of patents dealing wiht gut microbes and health. If there are other authors, they declare that they have no known competing financial interests or personal relationships that could have appeared to influence the work reported in this paper.

Acknowledgments

The authors would like to thank Prof. T. Michiels and Belén Lizcano-Perret for providing scientific support for tumor cell transduction with the plasmid TM915; Rose-Marie Goebbels and Caroline Bouzin for the technical support (Scann II and Halo® software) and realization of HE and the IREC 2IP. PDC is honorary research director FNRS.

Appendix A. Supplementary data

Supplementary data to this article can be found online at https://doi.org/10.1016/j.heliyon.2024.e33356.

References

[1] Y. Yan, et al., Chemiluminescence and bioluminescence imaging for Biosensing and therapy: in vitro and in vivo perspectives, Theranostics 9 (14) (2019) 4047–4065.
[2] N. Alsawaftah, et al., Bioluminescence Imaging Applications in Cancer: A Comprehensive Review, vol 14, IEEE Rev Biomed Eng, 2021, pp. 307–326.
[3] S. Iwano, et al., Single-cell bioluminescence imaging of deep tissue in freely moving animals, Science 359 (6378) (2018) 935–939.
[4] A. Mehle, Fiat Luc: bioluminescence imaging reveals in vivo viral replication dynamics, PLoS Pathog. 11 (9) (2015), 1005081.
[5] M.P. Hall, et al., Click beetle luciferase mutant and near infrared naphthyl-luciferins for improved bioluminescence imaging, Nat. Commun. 9 (1) (2018) 132.
[6] M. Bausart, et al., Mismatch between bioluminescence imaging (BLI) and MRI when evaluating glioblastoma growth: lessons from a study where BLI suggested "regression" while MRI showed "progression", Cancers 15 (6) (2023).
[7] A.M. Ansari, et al., Cellular GFP toxicity and immunogenicity: potential confounders in in vivo cell tracking experiments, Stem Cell Rev Rep 12 (5) (2016) 553–559.
[8] C.A. Grzelak, et al., Elimination of fluorescent protein immunogenicity permits modeling of metastasis in immune-competent settings, Cancer Cell 40 (1) (2022) 1–2.
[9] C.A. Grzelak, C.M. Ghajar, Elimination of 4T1 mammary tumor cells by BALB/cBy UBC-GFP transgenics following stable inheritance of the H-2b MHC allele, Immunohorizons 7 (1) (2023) 64–70.
[10] D.F. Quail, J.A. Joyce, Microenvironmental regulation of tumor progression and metastasis, Nat. Med. 19 (11) (2013) 1423–1437.
[11] M. Zabala, et al., Evaluation of bioluminescent imaging for noninvasive monitoring of colorectal cancer progression in the liver and its response to immunogene therapy, Mol. Cancer 8 (2009) 2.
[12] A. Rotermund, et al., Luciferase expressing preclinical model systems representing the different molecular subtypes of colorectal cancer, Cancers 15 (16) (2023).

[13] S. Wu, et al., A novel axis of circKIF4A-miR-637-STAT3 promotes brain metastasis in triple-negative breast cancer, Cancer Lett. 581 (2024) 216508.
[14] D.A. Lawson, et al., Tumour heterogeneity and metastasis at single-cell resolution, Nat. Cell Biol. 20 (12) (2018) 1349–1360.
[15] T. Biswas, et al., Attenuation of TGF-β signaling supports tumor progression of a mesenchymal-like mammary tumor cell line in a syngeneic murine model, Cancer Lett. 346 (1) (2014) 129–138.
[16] M. Blackman, et al., Mitochondrial protein Cox7b is a metabolic sensor driving brain-specific metastasis of human breast cancer cells, Cancers 14 (18) (2022).
[17] F. Sorgeloos, et al., A case of convergent evolution: several viral and bacterial pathogens hijack RSK kinases through a common linear motif, Proc. Natl. Acad. Sci. U. S. A. 119 (5) (2022).
[18] A. Follenzi, et al., Gene transfer by lentiviral vectors is limited by nuclear translocation and rescued by HIV-1 pol sequences, Nat. Genet. 25 (2) (2000) 217–222.
[19] E. Martinez-Salas, R. Francisco-Velilla, J. Fernandez-Chamorro, A.M. Embarek, Insights into structural and mechanistic features of viral IRES elements, Front. Microbiol. 8 (2017) 2629.
[20] B. Lizcano-Perret, et al., Cardiovirus leader proteins retarget RSK kinases toward alternative substrates to perturb nucleocytoplasmic traffic, PLoS Pathog. 18 (12) (2022), 1011042.
[21] B.C. Ahn, Applications of molecular imaging in drug discovery and development process, Curr. Pharmaceut. Biotechnol. 12 (4) (2011) 459–468.
[22] J.E. Kim, S. Kalimuthu, B.C. Ahn, Nucl med mol imaging, In vivo cell tracking with bioluminescence imaging 49 (1) (2015) 3–10, https://doi.org/10.1007/s13139-014-0309-x.
[23] T.V. Brennan, et al., Generation of luciferase-expressing tumor cell lines, Bio Protoc 8 (8) (2018).
[24] L. Naldini, et al., In vivo gene delivery and stable transduction of nondividing cells by a lentiviral vector, Science 272 (5259) (1996) 263–267.
[25] M. Nogawa, et al., Monitoring luciferase-labeled cancer cell growth and metastasis in different in vivo models, Cancer Lett. 217 (2) (2005) 243–253.
[26] R.M. Hoffman, Application of GFP imaging in cancer, Lab. Invest. 95 (4) (2015) 432–452.
[27] C. Schultheiss, M. Binder, Overcoming unintended immunogenicity in immunocompetent mouse models of metastasis: the case of GFP, Signal Transduct. Targeted Ther. 7 (1) (2022) 68.
[28] D. Rusciano, Differentiation and metastasis in melanoma, Crit. Rev. Oncog. 11 (2) (2000) 147–163.
[29] A.A. Jitariu, et al., Triple negative breast cancer: the kiss of death, Oncotarget 8 (28) (2017) 46652–46662.
[30] O.S. Blomberg, L. Spagnuolo, K.E. de Visser, Immune regulation of metastasis: mechanistic insights and therapeutic opportunities, Dis Model Mech 11 (10) (2018).
[31] C.H. Johnson, et al., Luciferase does not alter metabolism in cancer cells, Metabolomics 10 (3) (2014) 354–360.
[32] A.A. Khalil, et al., The influence of hypoxia and pH on bioluminescence imaging of luciferase-transfected tumor cells and xenografts, Int J Mol Imaging (2013) 287697, 2013.
[33] M.T. Haider, et al., Comparison of ex vivo bioluminescence imaging, Alu-qPCR and histology for the quantification of spontaneous lung and bone metastases in subcutaneous xenograft mouse models, Clin. Exp. Metastasis 41 (2) (2024) 103–115.
[34] S. Christoph, et al., Bioluminescence imaging of leukemia cell lines in vitro and in mouse xenografts: effects of monoclonal and polyclonal cell populations on intensity and kinetics of photon emission, J. Hematol. Oncol. 6 (2013) 10.